Available online at www.sciencedirect.com
SCIENCE DIRECT®
Catalysis Today 98 (2004) 575–581
CATALYSIS TODAY
www.elsevier.com/locate/cattod

Highly active and stable Rh/MgO–Al_2O_3 catalysts for methane steam reforming

Y. Wang[a,*], Y.H. Chin[a], R.T. Rozmiarek[a], B.R. Johnson[a], Y. Gao[a], J. Watson[b], A.Y.L. Tonkovich[b], D.P. Vander Wiel[a]

[a]*Pacific Northwest National Laboratory, P.O. Box 999, MSIN:K8-93, Richland, WA 99352, USA*
[b]*Velocys, 7950 Corporate Blvd, Plain City, OH 43064, USA*

Abstract

Highly active and coke-resistant Rh catalysts were developed for methane steam reforming in microchannel chemical reactors. Rh loading was optimized on a stable MgO–Al_2O_3 support to improve the volumetric productivity for methane conversion. Catalyst activities were stable over a wide range of steam/carbon ratios. In particular, experimental results demonstrated that Rh/MgO–Al_2O_3 catalysts are extremely active for methane steam reforming and are resistant to coke formation at stoichiometric steam/carbon ratio of 1 for over 14 h time-on-stream with no sign of deactivation. Methane steam reforming activities on this catalyst is compared in both a microchannel reactor and a conventional micro-tubular reactor. Significant performance enhancement was observed in microchannel reactors owing to improved heat and mass transfer.

Keywords: Methane steam reforming; Rh/MgO–Al_2O_3 catalyst; Microchannel reactor

1. Introduction

Methane steam reforming is a major commercial process for syngas production for fuel/chemical synthesis and hydrogen production [1]. The reaction is highly endothermic and is favored at low pressures. Conventional methane steam reforming processes suffer severe mass and heat transfer limitation, and the effectiveness factors of catalysts are typically less than 5% [2]. Microchannel reaction technology, which have been developed over the past decade [3,4], provides a potential breakthrough solution to the challenge of methane steam reforming processes. Microchannel reactors have a sandwich-like multi-layer structure consisting of a large number of closely spaced channels with a gap of less than 1 mm, which reduces heat and mass transport distance and thus enhancing the overall efficiency. Consequently, microchannel reactors allow process intensification and unprecedented temperature control. Heat transfer coefficients in microchannel reactors are as high as 10,000–35,000 W/m^2 K [5,6] compared to 100–700 W/m^2 K [7–9] in conventional reactors. Such high heat transfer coefficients coupled with the high surface-to-volume ratio achievable in microchannel reactors permit the operation of highly endothermic methane steam reforming at near isothermal conditions and provide the potential to significantly improve the efficiency of methane steam reforming process.

To fully take the heat and mass transfer advantages of microchannel reaction technology so that a greater volumetric productivity can be achieved, there is a need to develop highly active and stable methane steam reforming catalysts. To date, commercial methane steam reforming catalysts are based on Ni (∼12–20% Ni as NiO) supported on refractory material (e.g. α-alumina) doped with a variety of promoters [10]. Promoters such as potassium [11], calcium [12], and/or magnesium [13,14] alkali ions are added to serve as suppressants to retard carbon deposition on the catalyst. Although stoichiometry of methane steam reforming only requires 1 mol water/mol methane, excess steam (steam to carbon ratio of 2.5–3) [15] is used to reduce the by-product carbon formation. The use of excess steam

* Corresponding author. Tel.: +1 509 376 5117; fax: +1 509 376 5106.
E-mail address: yongwang@pnl.gov (Y. Wang).

0920-5861/$ – see front matter © 2004 Published by Elsevier B.V.
doi:10.1016/j.cattod.2004.09.011

burdens process economics due to higher energy demands. Additionally, downstream processes such as methanol synthesis and oxo-synthesis require high CO/CO_2 ratios in the reformate which are thermodynamically limited under high steam/carbon ratio. Precious metals are more active, in general, and are less prone than nickel to coke formation for methane steam reforming. Turnover numbers have been reported, relative to Ni, for silica based catalysts [16]: Rh (1.6) > Ru (1.4) > Ni (1) > Pd (0.6) > Pt (0.5).

The current work focuses on the development of Rh catalysts with the objective to improve the volumetric productivity of methane steam reforming in microchemical reactor while maintaining catalyst stability without use of excess steam.

2. Experimental

2.1. Synthesis and characterization

A series of $Rh/MgO–Al_2O_3$ catalysts with varying Rh loadings (1, 5, and 10 wt%) and 6 wt% MgO were prepared by an incipient wetness method. The as-received gamma Al_2O_3 (Engelhard AL 3945, 225 m^2/g) was first crushed and sieved to 70–100 mesh, then calcined at 5 °C/min to 500 °C, followed by holding isothermally at 500 °C for 2 h. Following the calcinations, an aqueous solution of magnesium nitrate hexahydrate (Aldrich, 99+%) was impregnated onto the calcined alumina then dried under vacuum at 110 °C for 8 h and calcined at 900 °C for 2 h. The resulting $MgO–Al_2O_3$ was further impregnated with Rh nitrate solution (Engelhard, 10.53 wt% Rh), then dried at 110 °C and calcined at 500 °C for 3 h. All calcinations mentioned above were conducted in a muffler furnace under atmospheric conditions. The as-synthesized catalysts were used in all powder catalyst activity testings.

Engineered catalyst activity was evaluated in a microchannel configuration. FeCrAlY felts (Porvair, Hendersonville, NC) with dimensions of 0.01 in. × 0.35 in. × 2 in. were used as the substrates for wash-coating the catalyst. FrCrAlY felts were first heat treated at 900 °C for 2 h at a rapid ramping rate of 20 °C/min. As previously shown [17,18], heat treatment at high temperature under an oxidizing environment facilitates the migration of Al species from the bulk FeCrAlY alloy substrate to the surface, which is subsequently oxidized to form a native aluminum oxide layer. Powder catalysts, prepared according to the method aforementioned, was ball-milled into aqueous catalyst slurry with a water to catalyst powder weight ratio of 8 to 1 on a wet milling setup for 24 h. The catalyst particles in the slurry, as measured by particle size analysis, was 1–3 μm. 0.065 g of catalyst was wash-coated onto 0.35 in. × 2 in. FeCrAlY felt with a thickness of 0.01 in., followed by drying and calcination at 500 °C for 2 h.

Rh dispersion was determined using static volumetric H_2 chemisorption methods performed in RXM-100 advanced catalyst characterization system (ASDI, Inc.) at room temperature. Catalysts were first reduced in situ under pure H_2 at 350 °C for 2 h followed by evacuation at 350 °C for 30 min. Transmission electron microscopy analysis was conducted on a JEOL 2010 high-resolution analytical electron microscope operating at 200 kV with a LaB_6 filament. The instrument is equipped with an X-ray energy dispersive spectrometry (EDS). To analyze the potential carbon deposition during methane steam reforming using TEM/EDS, spent catalyst was mounted on a Cu grid without Formvar/carbon support film.

2.2. Methane steam reforming activity testing

Methane steam reforming activity was tested in a 4 mm ID quartz microcatalytic reactor as well as a single channel device made from Inconel 625 with dimensions of 0.03 in. × 0.35 in. × 2.0 in. heated using a Thermcraft clam-shell furnace. For powder catalyst testing, 100 mg of catalyst powder at 70–100 mesh was used with alpha-alumina of similar size as diluent at a weight ratio of 4:1 (alumina to catalyst). A mixture of methane and water (varying steam to carbon molar ratios) was introduced at contact times varying from 1 to 25 ms. Here, contact time is defined as the catalyst bed volume divided by the volumetric inlet gas flowrate at standard temperature and pressure. Methane was controlled via Matheson 8272 or Brooks 5850E mass flow controllers. Water was introduced using a Cole-parmer 74900 series syringe pump for ambient experiments and by an Acuflow Series III HPLC pump for pressurized testing. Inconel sheathed type K thermocouples were utilized for temperature measurement in the catalyst bed, preheating zone, vaporizer and outlet. No-shock pressure transducers were used at both the upsteam and downstream positions for pressure measurement. Reactant and product gases were monitored online with Agilent Quad Micro GC equipped with a 5A PLOT (MS-5A), PoraPLOTQ, PoraPLOTU, OV-1 columns and thermal conductivity detectors.

3. Results and discussions

3.1. The effects of Rh loading

As described in Section 1, recent advancements in the microchemical chemical reactors have demonstrated the potential to significantly reduce transport limitations and hence improving catalyst effectiveness factor. High catalyst effectiveness factor allowed significant reduction in the mass of catalyst used in microchannel reactor while maintaining similar throughput attainable in a conventional reactor. Therefore, Rh concentration can be optimized over a wider range than conventionally practiced to improve the volumetric productivity without much cost concerns associated with the use of high Rh loadings.

A series of $Rh/MgO–Al_2O_3$ catalyst with Rh loadings of 1, 5, and 10 wt.% in the form of 70–100 mesh powder were

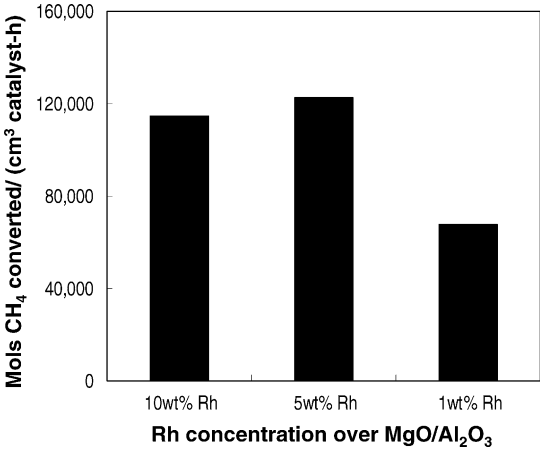

Fig. 1. Effect of Rh loadings over volumetric activity for methane steam reforming on Rh/MgO–Al_2O_3 catalysts (830 °C, 12 atm, steam/carbon ratio = 2, contact time = 1.9 ms).

prepared and tested in an Inconel single channel catalyst testing device as described in Section 2. Unlike conventional quartz microcatalytic fixed bed reactor, the single channel configuration coupled with diluted catalyst bed provides activity measurements under minimal transport artifacts. Methane steam reforming activity on these catalysts was measured over an 8 h period at 830 °C with a steam/carbon ratio of 2 at a contact time of 1.9 ms. To observe potential deactivation, catalysts were tested below equilibrium CH_4 conversion. Under these conditions, neither deactivation nor detectable pressure drop due to carbon formation was observed over the entire testing period.

Methane steam reforming activities for these catalysts were compared on a volumetric productivity basis, expressed in moles of CH_4 converted per unit volume of catalyst per hour, as presented in Fig. 1. Apparently, volumetric productivity for methane steam reforming was significantly increased with increasing Rh loading from 1 to 5 wt.%. Further increase in Rh loading from 5 to 10 wt.% only resulted in minimal improvement. Packing densities for all three samples are essentially the same, leading to a similar trend when comparing on a weight hourly space velocity (WHSV) basis.

Table 1
Dispersion and crystallite size on Rh/MgO–Al_2O_3 determined from volumetric H_2 chemisorption after in situ reduction at 350 °C

Catalyst	Dispersion (%)	Crystallite size (nm)
1 wt.% Rh/6 wt.% MgO–Al_2O_3	22.9	6.3
5 wt.% Rh/6 wt.% MgO–Al_2O_3	14.6	8.9
10 wt.% Rh/6 wt.% MgO–Al_2O_3	9.8	15.3

To investigate effects of Rh particle size on methane steam reforming, Rh particle sizes in the 1, 5, and 10 wt.% Rh catalysts were measured using volumetric H_2 chemisorption at room temperature, and the results are summarized in Table 1. The Rh particle sizes measured by the volumetric H_2 chemisorption were further verified by TEM analysis. Fig. 2a and b shows the representative TEM micrographs of a 5 wt.% Rh/MgO–Al_2O_3 sample. From TEM analysis, Rh dispersed on the MgO–Al_2O_3 support have the particle sizes ranging between 4 and 9 nm, in agreement with H_2 chemisorption measurement. One must recognize that the Rh crystallite size determined over fresh catalyst sample does not necessarily resemble that of working catalyst in methane steam reforming reactor under hydrothermal conditions. For this reason, we analyzed a spent 5 wt.% Rh (not shown here) after steam reforming reaction at 850 °C to determine the potential growth of Rh crystallite over the course of activity measurement. TEM analysis indicated that the spent catalyst contained Rh with similar particle size distribution without significant sintering, most likely due to low initial dispersion of Rh on the sample. Over the course of obtaining the forward turnover rate during an 8 h reaction period, as presented in the following section, Rh seems to be stable.

CH_4 steam reforming is an equilibrium limited reaction. The measured net reaction rate is influenced by the contact time. To remove the effect of contact time, forward turnover rates of CH_4 steam reforming were calculated using method recently reported by Wei and Iglesia [19] where the experimental conversion data and fractional distance from equilibrium along with H_2 chemisorption result are included in the calculation. Fig. 3 shows the calculated CH_4 steam

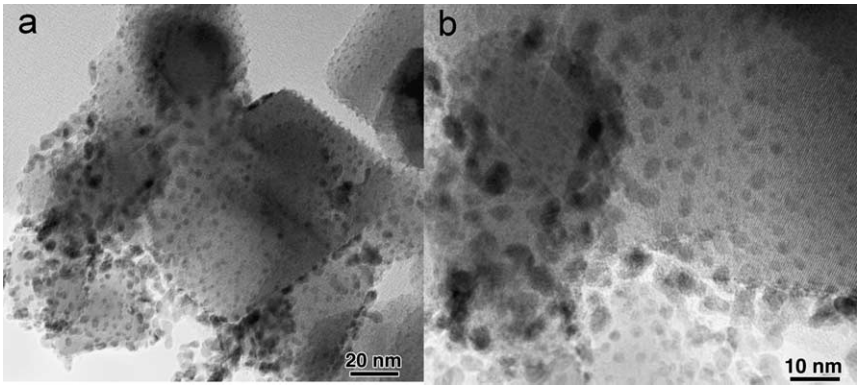

Fig. 2. Transmission electron micrograph (TEM) of 5 wt.% Rh/MgO–Al_2O_3 catalyst.

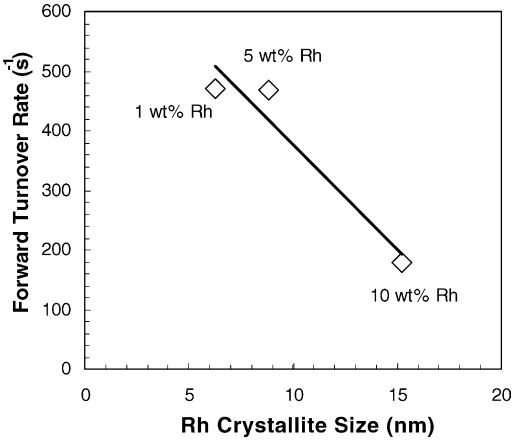

Fig. 3. Forward TOF as a function of Rh crystallite size (830 °C, 12 atm, steam/carbon ratio = 2, contact time = 1.9 ms, Al_2O_3/catalyst dilution = 4:1).

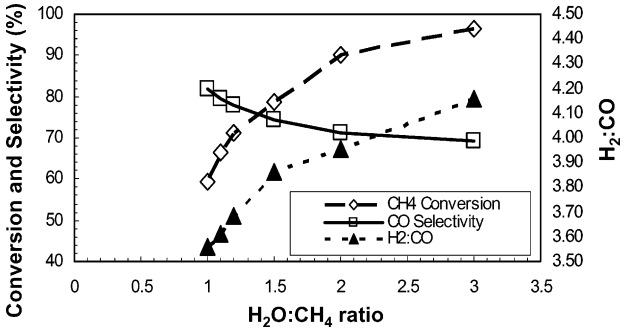

Fig. 4. Methane conversion, CO selectivity and H_2/CO ratio in the reformate over 10 wt.% Rh/MgO–Al_2O_3 (900 °C, 1 atm, contact time = 27 ms).

reforming forward turnover rates with Rh crystallite sizes. CH_4 turnover rate appears to be monotonically decreased with increasing Rh crystallite size over the crystalline size range studied (5–15 nm). The trend further supports the structure sensitivity of CH_4 steam reforming over noble metal, recently proposed by Wei and Iglesia [19] on metal clusters in the range of 1.5–6.5 nm. In their study, it was proposed that small metal crystallites with high surface concentration of coordinatively unsaturated sites are active for C–H activation, resulting in high turnover rates for steam reforming. It is noteworthy that although the 1 wt.% Rh/MgO–Al_2O_3 sample is not as active in terms of volumetric productivity as shown in Fig. 1, it exhibited a 2.5-fold increase in CH_4 turnover rate compared to 10 wt.% Rh/MgO–Al_2O_3.

3.2. Methane steam reforming on 10 wt.% Rh/MgO–Al_2O_3

As aforementioned, 5 wt.% Rh/MgO–Al_2O_3 showed significant improvement over 1 wt.% Rh//MgO–Al_2O_3 based on volumetric productivity, and similar performances were observed with 10 wt.% Rh//MgO–Al_2O_3. To exploit the heat and mass transfer advantages of microchannel reactors for improved volumetric productivity, catalysts with high Rh loadings (5–10 wt.%) were selected for microchannel applications [4,20,21]. Such Rh loadings are much higher than the previous work on precious metals (typically about 1 wt.% [19,22,23]) for methane steam reforming, in which the primary focus was on the optimization of metal dispersion, not necessarily on the enhancement of volumetric throughput. As shown in the previous section, high concentration of Rh with low metal dispersion exhibited significant enhancement in terms of reactor throughput. For application in microchannel steam reformer, the present work focused on evaluating performances of 10 wt.% Rh/MgO–Al_2O_3 catalyst tested in both powdered and engineered forms.

The process of methane steam reforming is most economical when performing under a stoichoimetric carbon to steam ratio of 1. It is well recognized that catalysts deactivate rapidly under low steam/carbon ratios due to deposition of graphitic carbon on catalyst surfaces [1,15]. The methane steam reforming reaction is typically carried out at a steam/carbon ratio of at least 2.5 to minimize coke formation. Such a ratio is undesirable due to a larger required reactor volume and steam recycling associated with the use of extra steam. Additionally, the high steam/carbon ratio results in syngas with a higher H_2/CO ratio which is not desirable for methanol and Fischer–Tropsch synthesis. Therefore, 10 wt.% Rh/MgO–Al_2O_3 catalyst was tested over a wide range of steam/carbon ratios (1–3) at 900 °C and a contact time of 25 ms. The objective was to evaluate the catalyst stability at various steam/carbon ratios. Again, methane conversions were kept below equilibrium conversion so that any noticeable catalyst deactivation can be readily identified. The experiment started with a steam/carbon ratio of 3 and the steam/carbon ratio was gradually reduced when no noticeable deactivation or change in pressure drop were observed. Methane flowrate was increased with decreasing steam/carbon ratio to maintain a constant total flowrate. Fig. 4 shows the methane conversion, CO selectivity, and H_2/CO ratio as a function of steam/carbon ratio. Methane conversion and H_2/CO ratio increase with steam/carbon ratio, while CO selectivity decreases with increasing steam/carbon ratio. The decreased CO selectivity with increasing steam/carbon ratio is likely due to enhanced water-gas-shift reaction rate at higher steam concentrations.

During the course of experiments of approximately 8 h, no noticeable deactivation was observed even at a steam/carbon ratio of 1, leading to the further evaluation of stability of 10 wt.% Rh/MgO–Al_2O_3 at a stoichiometric steam/carbon ratio. Again, methane conversion was kept below thermodynamic equilibrium conversion so that any potential deactivation could be readily observed. The time-on-stream methane conversion and CO selectivity over the course of 14 h time-on-stream at stoichiometric steam/carbon ratio are shown in Fig. 5 with equilibrium

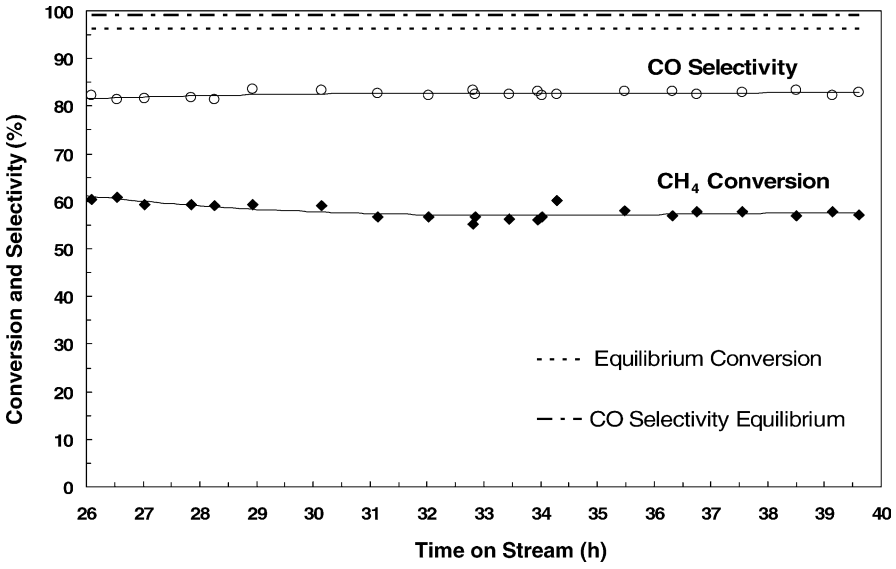

Fig. 5. Time-on-stream methane conversion and CO selectivity over 10 wt.% $Rh/MgO/Al_2O_3$ catalyst (900 °C, steam/carbon ratio = 1, 1 atm, contact time = 25 ms).

CH_4 conversion and CO selectivity included for reference purposes. Prior to exposing to stoichiometric steam/carbon feed, the catalyst was tested under higher steam/carbon ratios (not shown here) for 26 h with no noticeable deactivation. As illustrated in the figure, methane conversion and CO selectivity remain relatively constant over the course of 14 h activity testing under stoichiometric steam-to-carbon ratio, indicating no noticeable catalyst deactivation. After the experiment, the spent catalyst sample was mounted on a Cu supporting grid for TEM/EDS analysis. Fig. 6 shows TEM micrograph of the spent catalyst, EDS analysis over various areas on the sample confirms the absence of carbonaceous species on catalyst after reaction, further confirming that the 10 wt.% $Rh/MgO–Al_2O_3$ is stable and coke-resistant for methane steam reforming under stoichiometric steam/carbon ratio.

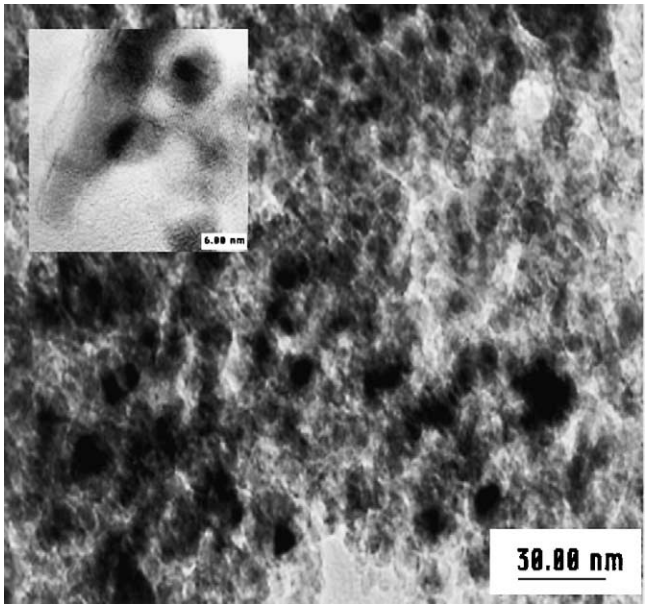

Fig. 6. TEM micrograph of spent 10 wt.% $Rh/MgO–Al_2O_3$ catalyst after CH_4 steam reforming for 14 h under a steam/carbon ratio of 1.

3.3. Methane steam reforming of 10 wt.% $Rh/MgO–Al_2O_3$ in a microchannel reactor

10 wt.% $Rh/MgO–Al_2O_3$ was further studied in an engineered form using a microchannel reactor. The

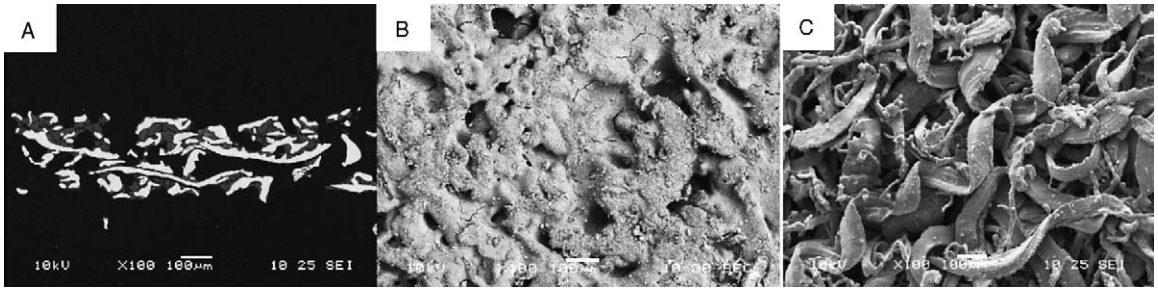

Fig. 7. Cross-section (A) and surface (B) SEM micrograph of a wash-coated 10 wt.% $Rh/MgO–Al_2O_3$ over FeCrAlY felt engineered catalyst. SEM of uncoated FeCrAlY surface (C) is included for reference.

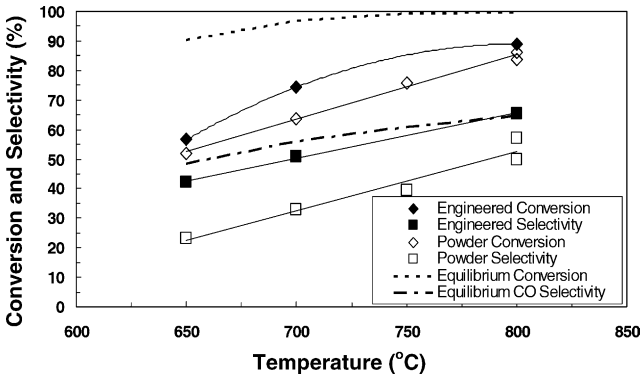

Fig. 8. Methane conversion and CO selectivity as a function of temperature: a comparison of engineered catalyst in a microchannel reactor vs. same powder catalyst (10 wt.% $Rh/MgO/Al_2O_3$) in a micro-tubular reactor under identical conditions (900 °C, 1 atm, steam to carbon ratio = 1, contact time = 27 ms).

engineered catalyst was prepared by coating the 10 wt.% $Rh/MgO–Al_2O_3$ catalyst on metal felt substrate surfaces as described in Section 2. Fig. 7 depicts the cross-section and surface view scanning electron micrographs of a wash-coated engineered catalyst. For reference purposes, surface micrograph of a bare FeCrAlY felt was included. As demonstrated in the micrograph, thin coating of catalyst powder dispersed onto the fibers coupled with large openings within the metal felt fiber (average pore size ~150 μm) in the engineered catalyst are anticipated to significantly reduce internal mass transfer resistance. In a typical testing, two felt engineered catalysts with identical dimensions (0.01 in. × 0.35 in. × 2 in.) were placed in the single channel reactor with a gap of about 0.01 in. Inside the channel, the engineered catalyst pieces remained compressed and in close contact with the reactor walls for improved heat transfer. Such an arrangement of engineered structures also has the advantage of negligible pressure drop even under very short contact time conditions. The engineered catalysts were again studied at a very short contact time of 25 ms (the entire catalyst chamber volume including the felt and gap volume were used for the calculation of contact time).

Fig. 8 shows the CH_4 conversion and CO selectivity as a function of temperature at a steam/carbon ratio of 3. For comparison purposes, the results of powdered catalysts in a conventional micro-tubular reactor under identical experimental conditions were included in the figure. As shown in Fig. 8, over the entire temperature range studied, engineered catalysts exhibited higher methane conversion and CO selectivity than powdered catalysts, possibly due to enhanced mass and heat transfer in engineered catalyst structures. The higher CO selectivity in engineered catalysts also supports the fact that higher average catalyst bed temperature or lower temperature gradients existed in the engineered catalysts due to improved heat transfer because CO selectivity is thermodynamically favored at high temperatures. Since catalyst weight used in micro-tubular reactor in the experiment is a factor of 2.2 times higher than that used in the engineered catalyst testing, we likely underestimate the performances of engineered catalysts. In another word, much higher CH_4 conversion and CO selectivity are anticipated if both catalysts are compared under identical weight hourly space velocity (WHSV).

4. Conclusions

Highly active and stable $Rh/MgO–Al_2O_3$ catalysts were developed for methane steam reforming using microchannel reactors. Catalysts developed are extremely active as indicated by high methane conversions at short contact times. Experimental results also showed that the catalysts exhibited excellent coke resistance even under a stoichiometric steam/carbon ratio of 1. Rh clearly showed the structure sensitivity towards methane steam reforming over the range of Rh crystalline size examined. The 10 wt.% $Rh/MgO–Al_2O_3$ catalyst, among the ones showing highest volumetric productivity for methane steam reforming, was also evaluated in an engineered structure in a microchannel reactor. The enhanced heat and mass transfer of engineered catalysts results in improved performances of methane steam reforming.

Acknowledgements

This work was performed in the Environmental Molecular Science Laboratory, a national scientific user facility sponsored by the U.S. Department of Energy's Office of Biological and Environmental Research and located at Pacific Northwest National Laboratory in Richland, WA.

References

[1] J.R. Rostrup Nielsen, Catalytic Steam Reforming, Danish Technical Press, 1984.
[2] A.M. Adris, B.B. Pruden, C.J. Lim, J.R. Grace, The Can. J. Chem. Eng. 74 (4) (1996) 177.
[3] R.S. Wegeng, M.K. Drost, C.E. McDonald, U.S. Patent 5,611,214.
[4] A.L.Y. Tonkovich, Y. Wang, S.P. Fitzgerald, J.L. Marco, G.L. Roberts, D.P. Vander Wiel, R.S. Wegeng, US 6,488,838.
[5] A.L.Y. Tonkovich, C.J. Call, D.M. Jimenez, R.S. Wegeng, M.K. Drost, AIChE Symp. Ser., vol. 92, No. 310, AIChE, New York, 1996, p. 119.
[6] B. Thonon, P. Mercier, in: Proceedings of the Second International Conference on Proc. Intensif. in Pract., vol. 28, BHR Group, London, 1997, p. 49.
[7] H.J. Bock, O. Molerus, in: J.R. Grace, J.M. Matsen (Eds.), Fluidization, Plenum Press, New York, 1980, p. 217;
H.J. Bock, O. Molerus, German Chem. Eng. 5 (1983) 57.
[8] H. Seko, S. Tone, T. Otake, in: D. Kunii, R. Toei (Eds.), Fluidization, Engineering Foundation, New York, 1983, p. 331.
[9] G.F. Froment, K.B. Bischoff, Chemical Reactor Analysis and Design, 2nd ed. Wiley, 1990.

[10] J.R. Rostrup-Nielsen, in: J.R. Anderson, M. Boudart (Eds.), Catalysis, Science and Technology, vol. 5, Springer-Verlag, Berlin, 1984, Chapter 1.
[11] M.V. Twigg (Ed.), Catalyst Handbook, Wolfe, London, 1989.
[12] Z. Zhang, X.E. Verykios, Appl. Catal. A: Gen. 138 (1996) 109.
[13] O. Yamazaki, K. Tomishige, K. Fujimoto, Appl. Catal. A: Gen. 136 (1996) 49.
[14] T. Borowiecki, Appl. Catal. 10 (1984) 273.
[15] J.N. Armor, Appl. Catal. A: Gen. 176 (1999) 159.
[16] E. Kikuchi, E. Tanaka, Y. Yamazaki, Y. Morita, Bull. Jpn. Petro. Inst. 16 (1974) 95.
[17] Y. Wang, Y.H. Chin, Y. Gao, U.S. Patent 6,713,519.
[18] C. Badini, F. Laurella, Surf. Coat. Technol. 135 (2001) 291.
[19] J. Wei, E. Iglesia, J. Phys. Chem. B 108 (2004) 4094.
[20] Y. Wang, R. Dagle, Y. Chin, D. Palo, J. Hu, J. Holladay, Prepr.-Am. Chem. Soc., Div. Pet. Chem. 47 (1) (2002) 114–115.
[21] A.L.Y. Tonkovich, Y. Wang, S.P. Fitzgerald, J.L. Marco, G.L. Roberts, D.P. Vander Wiel, R.S. Wegeng, US 6,680,044.
[22] T. Maillet, J. Barbier Jr., P. Gelin, H. Praliaud, D. Duprez, J. Catal. 202 (2001) 367.
[23] K. Nagaoka, K. Seshan, K. Aika, J.A. Lercher, J. Catal. 197 (2001) 34.